Subcooling on flow boiling critical heat flux enhancement of Cr-coated tube under low pressure

Namgook Kim [a], Geon Young Byun, Bumjin Jung, Sung Joong Kim [a, b*]
[a]*Hanyang University, 222 Wangsimri-ro, Seongdong-gu, Seoul 04763, Republic of Korea*
[b]*Institute of Nano Science & Technology, Hanyang University*
[*]*Corresponding author: sungjkim@hanyang.ac.*

1. Introduction

The development of accident-tolerant fuel (ATF) cladding has highlighted the need for surface coating techniques that can be applied to existing zirconium-based alloys. These coatings offer numerous advantages, including high neutron efficiency and a short development time. Furthermore, coating processes offer the potential to improve boiling heat transfer, especially critical heat flux (CHF) [1-2]. This is because the coating's micro/nanoscale structures promote capillary wicking, which is a crucial aspect of bubble dynamics and flow boiling CHF [3]. Therefore, this study aimed to assess the impact of modified surface structures resulting from the ATF coating process on flow boiling performance.

2. Experiment

2.1 Sample preparation and surface morphology

To prepare the test tubes, we followed a three-step fabrication process: grinding, cleaning, and deposition. We used sandpaper to roughen the tube surface, as surface roughness can strongly affect CHF. Next, we cleaned the tube with ethanol and deionized water using an ultrasonic cleaner. These first two steps also served as the preparation procedure for the bare tube. Then, we used DC magnetron sputtering to deposit an ATF candidate material, Chromium (Cr), onto the Zr-based alloy tube. Table I lists the selected coating conditions for creating nanoscale surface structures based on a structure zone model [4].

Table I: Sputtering conditions for DC magnetron sputtering

Sputtering conditions	Characteristics
Exposure environment	99.95% pure Cr
Substrate temperature (ºC)	150
Exposure time (hr)	1
Working pressure (torr.)	1×10^{-2}
DC power (W)	150-160
Sputtering gas	100% Ar

The SEM (Scanning Electron Microscopy; Apreo S Hivac) was used to analyze the surface morphology of the fabricated tubes, as depicted in Fig. 1(a) and (b). Both tubes had uni-directional microscale scratches from the initial grinding process. On the Cr-coated tube, however, numerous dome-shaped particulate nanostructures were formed on top of the Cr-coated layer, as shown in the inset images. Fig. 1(c) and (d) display cross-sectional SEM images of the fabricated tubes with the milling process using an auto-polisher. The thickness of the Cr-coated layer was confirmed to be approximately 1.0 μm, with no significant defects in the fine columnar grains.

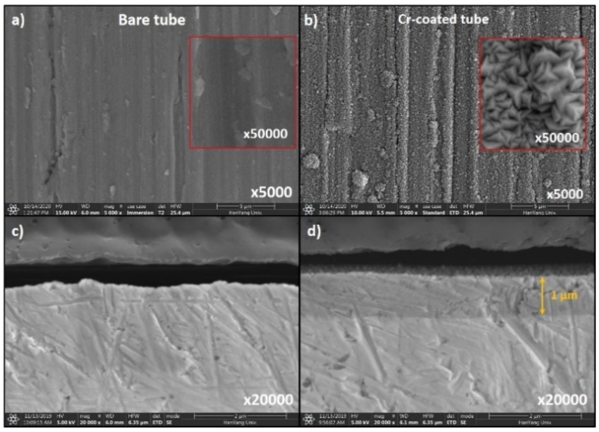

Fig. 1. SEM images of surface morphology on (a) bare tube and (b) Cr-coated tube and cross-sectional images (c) before and (d) after deposition of Cr layer.

2.2 Flow boiling experimental setup

A schematic of the forced convective flow boiling test loop is presented in Fig. 2(a). The test section consists of a boiling chamber, circulation pump, accumulator, preheater, buffer tank, shell & tube type condenser, and shell & tube type heat exchanger. Deionized water serves as the working fluid and is drawn from the buffer tank, then passed through a heat exchanger and pumped by a high-temperature centrifugal pump with a maximum operating temperature of 180°C. The coolant is heated in a preheater with a maximum output power of 20 kW, flows through the boiling chamber, and returns to the buffer tank. Data acquisition systems measure the flow rate, pressure, voltage, and temperature at each component. A 20 mm diameter PC tube forms an annular flow inside the boiling chamber.

Fig. 2(b) presents the detailed design of the test section used in this study. The test specimen is 3/8 in. in diameter and 120 mm in length, with a heated length of 100 mm. Both sides of the remaining 10 mm length are connected with copper electrodes to ensure adequate electrical contact. The Zr-based tube's electrical resistance is measured at 1.0 mΩ, which is considerably higher than the 0.0136 mΩ of copper. The inside of the test tube is insulated by a ceramic-type wool. Three K-type thermocouples are located inside the tube at heights of

25, 50, and 75 mm to monitor the inner wall temperature at each height. Pt wires are connected to both ends of the copper electrode rod to measure the voltage drop.

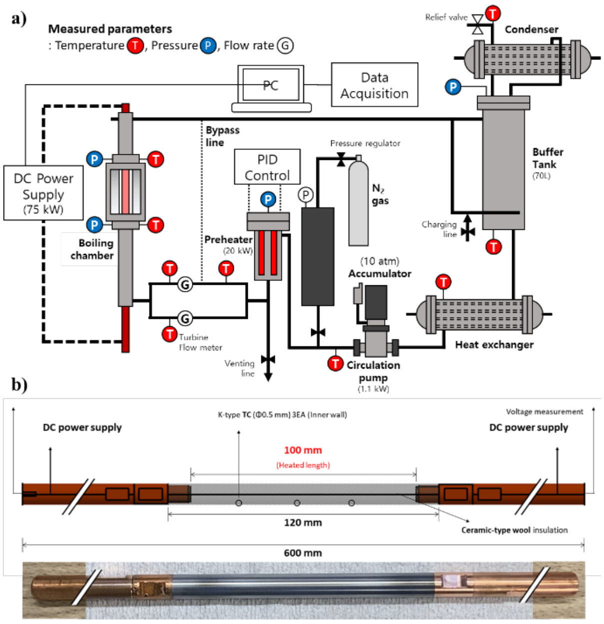

Fig. 2. Schematic diagram of (a) forced convective flow boiling test loop; (b) test section.

Table II: Flow boiling test condition

Test conditions	Characteristics
Test section	Vertical circular tube
Test section material	Zr-based alloy
Outer tube diameter	9.525 mm (3/8 in.)
Heated length	100 mm
Flow type	Annular flow
Outer annular diameter	20 mm
Hydraulic flow diameter	10.475 mm
Loop pressure (MPa)	0.131 (1 atm)
Inlet mass flux (kW/m^{2}s)	400
Subcooling Temp. (^{o}C)	20/40/60
Tube	Bare / Cr-coated

The experimental test conditions are presented in Table II. The tests were performed on both bare and Cr-coated tubes at fixed inlet mass flux (400 kg/m^{2}s) and inlet temperatures of 20/40/60°C under atmospheric pressure. To supply DC power to the test section, the direct Joule heating method was used. This method enables the stepwise provision of steady-state heat flux while controlling the current input. The following Joule's heat flux equation was used to calculate the applied heat flux.

$$q'' = \frac{Power}{A_{heated}} = \frac{VI}{\pi D L_{heated}} \qquad (1)$$

Here, V, I, D, and L_{heated} are the measured voltage drop across the test tube, the measured current, the tube outer diameter, and the heated length, respectively. Uncertainty of the measured heat flux was estimated as 5.2% based on the error propagation method. The maximum heat flux achievable in the test section is about 25 MW/m^2.

The DC power input was regulated by a heat flux interval of 100 kW/m^2, and steady-state was achieved by observing a surface temperature that remained constant for at least three minutes. The point at which the thermal flux difference over the surface temperature difference increased by more than 1% was considered the occurrence of CHF. The boiling curve in Fig. 3 represents the flow boiling experiment conducted in accordance with the experimental procedure.

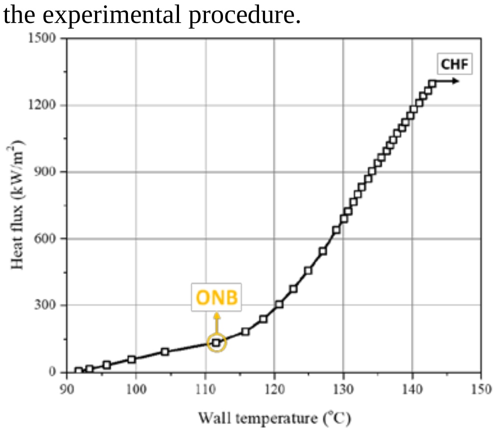

Fig. 4. Comparison of input and output power and calculated

The heat losses in the test section was calculated by using following normalized difference between the electrical input power and the fluid thermal power.

$$HL(\%) = \frac{VI - \dot{m}c_p(T_{outlet} - T_{inlet})}{VI} \times 100 \qquad (2)$$

Here, T_{outlet}, $\dot{m}$, and c_p are the measured chamber outlet temperature, inlet mass flow rate and the average specific heat of liquid between inlet and outlet temperature, respectively. Fig. 4 shows the input power, the fluid thermal power, and the calculated heat loss following experiment time. At high heat flux of interest in CHF experiment, the heat loss is less than 5%.

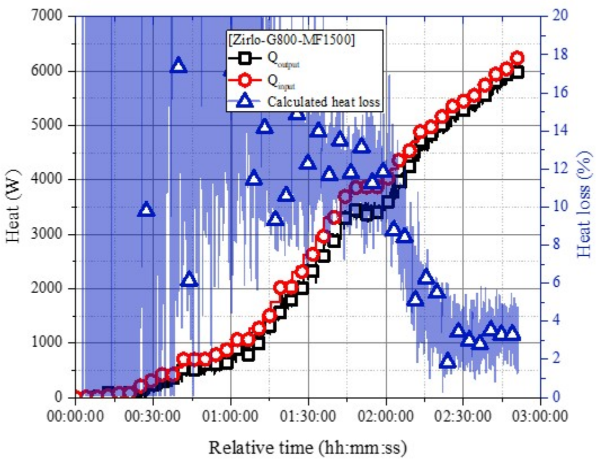

Fig. 5. Comparison of input and output power and calculated heat loss in the test section following the test time.

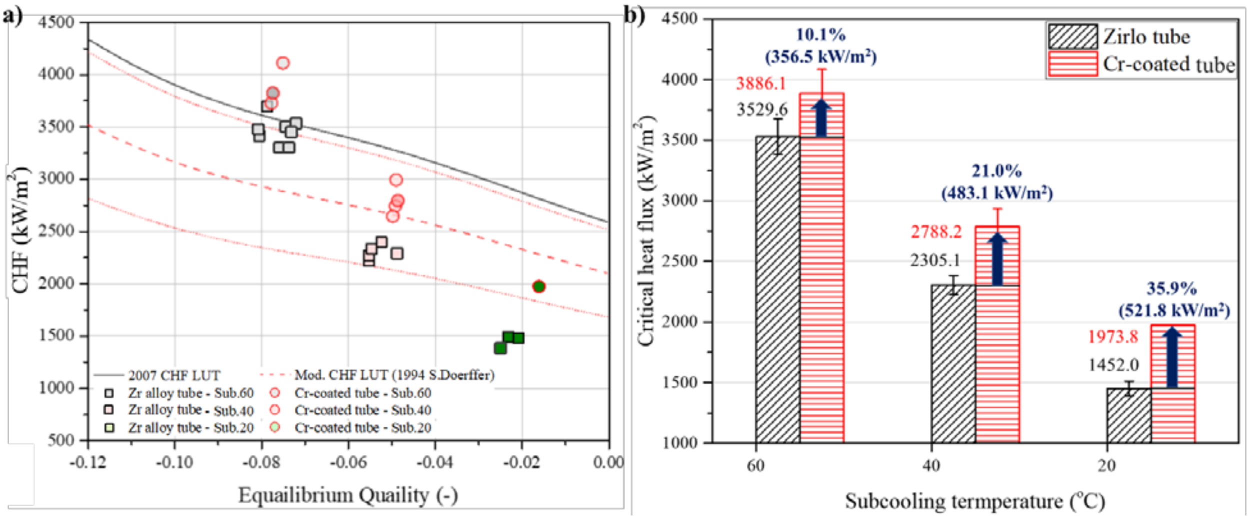

Fig 5. Flow boiling results: a) Flow boiling CHF following the calculated equilibrium quality, b) Comparison of CHF according to coated layer in each subcooling

3. Results and discussion

3.1 Flow boiling CHF experiment results

The results of flow boiling CHF on bare tubes and Cr-coated tubes are presented in Fig. 5(a) for a mass flux of 400 kg/m^{2}sec and subcooling temperatures of 20/40/60^{o}C. The subcooling temperatures were converted to equilibrium quality using equation (3), which provides a good measure of subcooling degree.

$$X_{exit} = \frac{c_p(T_{out} - T_{sat})}{h_{fg}} \quad (3)$$

Here, h_{fg} is the latent heat of water under 0.131 MPa.
The results showed that the effect of the coating process on flow boiling CHF varied significantly with the equilibrium quality. As the equilibrium quality decreased (i.e., subcooling temperature increased), the CHF enhancement due to the coated layer was amplified. This is because, with an increase in subcooling temperature, the bubbles departure diameter decreases, leading to a reduction in capillary flow rate and CHF enhancement. However, as the subcooling temperature decreases, bubble density tends to increase. Therefore, further analysis through observation of bubble dynamics may be necessary in the future.

4. Conclusion

In conclusion, this study aimed to evaluate the impact of modified surface structures resulting from the accident-tolerant fuel (ATF) cladding coating process on flow boiling performance. To achieve this, subcooled flow boiling experiments were conducted with Cr-coated tube by DC magnetron sputtering technique under atmospheric pressure at fixed flow condition of 20/40/60^{o}C inlet subcooling and 400 kg/m^{2}s mass flux. The study provides valuable insights into the use of surface coating techniques to enhance boiling heat transfer and improve nuclear reactor performance.

Acknowledgement

This research was supported by the National Research Foundation of Korea (NRF) grant funded by the Korean government (MSIP: Ministry of Science, ICT and Future Planning) (No. NRF-2020M2A8A5025124)

REFERENCES

[1] H.H. Son, Y.S. Cho and S.J. Kim, Experimental study of saturated pool boiling heat transfer with FeCrAl- and Cr-layered vertical tubes under atmospheric pressure, International Journal of Heat and Mass Transfer, Vol.128, p.418–430, 2019.
[2] N. Kim, H.H. Son and S.J. Kim, Oxidation effect on pool boiling critical heat flux enhancement of Cr-coated surface for accident-tolerant fuel cladding application, International Journal of Heat and Mass Transfer, Vol.144, 118655.
[3] J.H. Seong, C. Wang, B. Phillips and M. Bucci, Effect of PVD-coated chromium on the subcooled flow boiling performance of nuclear reactor cladding materials, Applied Thermal Engineering, Vol. 213, 118670.
[4] J.A. Thornton, Influence of apparatus geometry and deposition conditions on the structure and topography of thick sputtered coatings, Journal of Vacuum Science and Technology. Vol.11, p.666–670, 1974.
[5] K.H. Chu, R. Enright, E.N. Wang, Structured surfaces for enhanced pool boiling heat transfer, Appl. Phys. Lett. 100 (24) (2012) 241603.